Design and Fabrication of Dragonfly Test Bed for Aerodynamic Characterization

Yutong Wang, Shankar Kalyanasundaram
Department of Engineering
The Australian National University, Canberra, Australia
Yutong.Wang@anu.edu.au, Shankar.Kalyanasundaram@anu.edu.au
John Young
School of Mechanical, Civil and Aerospace Engineering
Australian Defence Force Academy, UNSW, Canberra, Australia
J.Young@adfa.edu.au

Abstract

This paper focuses on the design of an electro-mechanical device for studying the aerodynamic behavior of flapping wings. The experimental device is designed to mimic the flight behavior of dragon fly. Wing flapping speed is precisely controlled by controlling the motor speed. Wing flapping amplitude could be varied by changing the rotating arm length. Wing rotation amplitudes during down- and up- stroke could be different and are controlled separately by two different springs. A six degree of freedom sensor is placed at the wing root to collect the force and torque data. The test of a wing with a dragonfly hind-wing contour but enlarged 11 times, showed the device met the design expectation, and further more, the phase-averaged data for lift force in one flapping cycle had the similar pattern as the ones obtained via CFD simulations as well as the one calculated based on a real dragonfly's flight behavior.

1 Introduction

Micro-Air-Vehicles (MAV) is expected to play useful roles from military applications to inspection of commercial infrastructure in space or condition restricted areas. The scaled-down versions of the current existing aircraft are not the ideal candidates for applications, where flight at low speed, hovering ability and high maneuverability are needed. Hence, design of MAVs that mimic the flyers in Nature such as birds or insects becomes increasingly attractive. Compared to birds, insects have higher maneuverability and higher gust-tolerance, as well as higher aerodynamic efficiency. Therefore, studying insect-like flapping flight behavior could lead to insect-inspired MAVs particularly useful to be employed in non-open areas such as buildings, tunnels, caves, and flying longer with more payloads.

In contrast to the fixed wing flight, flapping flight principles belong to the regime of unsteady aerodynamics which has remained largely unknown. A dynamic scaled model, Robofly, was used to confirm the leading edge vortex (LEV) existence at low Reynolds number [Dickinson and Gotz, 1993]. Using the same model, it was reported that the rotational force during stroke reversal may provide a source for insect lift [Dickinson, 2004]. It was noted that by incorporating a Clap-and-Fling mechanism [Weis-Fogh, 1973] in the Robofly model, the lift could be enhanced by 17% [Lehman 2004; Sane, 2005]. By utilizing a model named Hawkmoth, it was found that LEV is the source for high lift and the twist and camber of wing have no significant effect on lift [Usherwood and Ellington, 2002]. It was noted that the phase difference in flapping between the fore- and hind- wings has no effect on fore-wing, but lift production in hind-wing may vary by a factor of two [Maybury and Lehman, 2004] . Double LEV was observed when carrying out experiment with a model flapping wing [Lu, Shen *et al.,* 2006]. One of the common features of all these experimental work is that the wing rotation angle during flapping was designed being actively imposed by either motor directly or some motor-driven mechanical mechanism. Although the wing rotation at any instant could be actively controlled by muscles in insects while flapping, it is more likely the wing rotates with the assistance of the torque caused by the wing inertia and the air force exerted on the wing. It was noticed that the wing rotation was caused by inertial effects [Ennos, 1988]. It was demonstrated by simulation and quasi-state analysis that the pronation and supination could be passive in dragonfly and fruit fly [Bergou *et al.,* 2007]. This implies that during the flapping motion, aerodynamic torque and wing inertia could have an influence on the wing rotation and hence the angle of attack (AOA) as well. This further implies that the wing rotation in insect flight during the flapping cycle could be due to the combined effect of aerodynamic forces on the wing, wing inertia and insect muscular control. If the flexibility of the wing is also taken into account, the degree of the rotation could be different at the different position along the main spar of the wing.

The wing rotation mechanism of the current test bench was designed to mimic the effects mentioned above and it is believed to be closer to the insect's wing rotation mechanism found in Nature.

The main focus of this paper is the design of a physical model (test bench) for insect flight study with passive wing

rotation concept. It is hoped that this test bench could produce useful experimental results to further the knowledge in unsteady aerodynamic research for this class of flight behavior. In addition, the test bench design itself and the experimental data collected might be able to provide some references for the design of future MAV with passively rotating wings.

2 Experimental Device Design

The designed experimental device was constructed with three main systems, namely mechanical, electrical and data acquisition system. The mechanical system includes the structure supporting for the entire device. It also contains the functional mechanism to convert the motor rotation motion to the wing flapping motion. In addition, it provides the control of angle of attack (AOA) for a passively rotating wing. The electrical system controls the flapping frequency accurately via a servo amplifier and a personal computer. Data acquisition system collects the force and torque data from a six degree of freedom (6-DOF) sensor placed at the root of the wing. The rotation angle of the wing root was measured via a Hall-effect sensor located at the end of the wing rotation shaft. The schematics of the experimental device are given in Figure 1 and Figure 2.

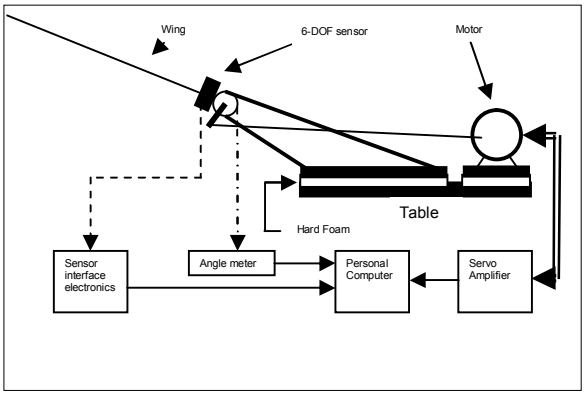

Figure 1: Schematic Diagram of the Experimental Device

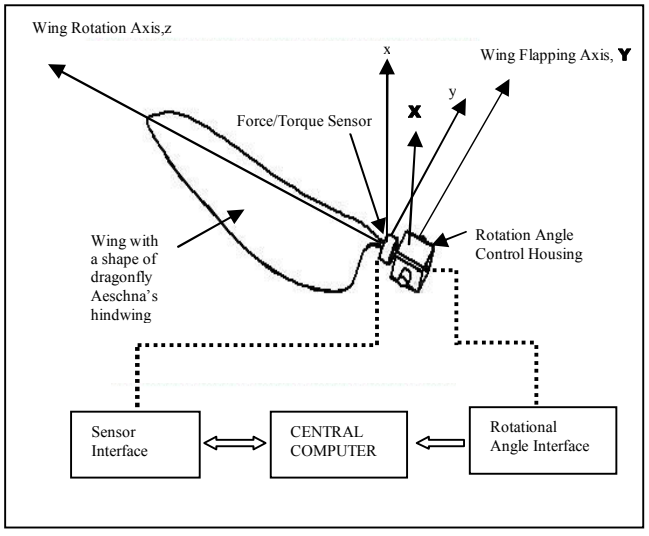

Figure 2: Top Rear View of the Device

2.1 Mechanical System Design

The mechanical system in the designed test bench includes three major assemblies: supporting structure, four-bar linkage mechanism and a mechanical unit for AOA control of the wing which rotates passively with the assistance of air pressure exerting on it and wing's own inertia.

2.1.1 Supporting Structure

In order to minimize the wobbling motion of the experimental device, a robust metal table was built to provide a solid foundation for the experiments. The whole flapping portion of the device was supported by a frame made of two aluminum plates and a thick base plate. The frame was bolted onto a solid timber. A big block of foam with 100mm thickness was placed and glued between the solid timber and the table for insulating the noise from motor-gearbox assembly to the sensor. Same strategy of using foam to insulate noise was employed under the motor. Data collected by 6-DOF sensor was so clean that low frequency pass filtering became unnecessary.

2.1.2 Four-Bar Linkage Mechanism

A four-bar mechanical structure was employed in the design to convert the motor's 360 degree rotational motion to wing flapping motion with the amplitude adjustable from 50 to 60 degree. The flapping amplitude can be adjusted by changing the length of the driving arm, which is formed by the flange fixed on the output shaft of the gearbox. There are a series of holes on the flange having different centre distances to the gearbox output shaft. Changing the length of the driving arm is achieved by selecting different holes on the flange.

Two ends of the linkage were tapped in opposition directions which made the length of the linkage adjustable, which in turn made the angle between the centre plane (the plane dividing the flapping angle in two equal halves, flapping angle is measured between the two extreme flapping positions of the wing main spar) and horizontal plane adjustable. Since the four-bar mechanism linked the gearbox and the flapping wing, it provided another path for transmitting the gearbox noise to the sensor located on the wing root. To cut off this noise path, the linkage was redesigned by using 3 sections (linkage_1, 2 and 3) and rubber was placed between 1 and 2, and 2 and 3. Figure 3 illustrates this mechanism.

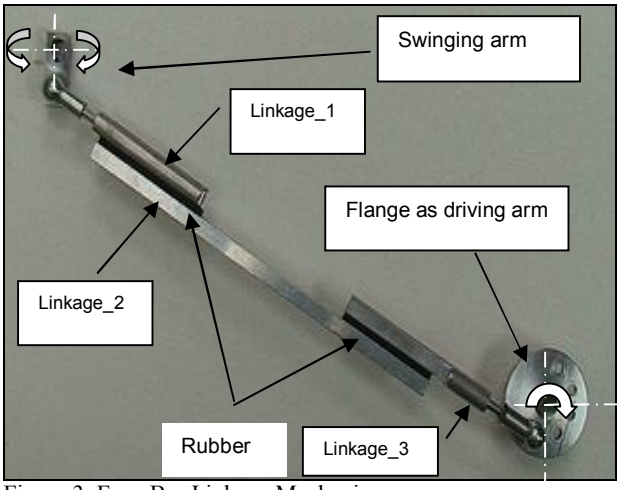

Figure 3: Four-Bar Linkage Mechanism

2.1.3 Wing Rotation Angle Control Unit

The AOA has an influence on both insect's lift and thrust, therefore its maneuverability. It is regarded as one of the important parameters in flight control. The experimental devices seen so far used motor or motor driven mechanical components to actively control the angle of attack during the whole wing rotation course. Active control mechanism inevitably made the control, design and device itself complex and less efficient in terms of power consumption. The current AOA control unit was designed to reflect the fact that the wing rotation is passive yet its overall rotating degree is controllable. The wing rotating motion partially determined by AOA control unit can be described as a sinusoidal-like motion with the same frequency as the one for wing flapping motion. Its amplitudes for up and down stokes were designed to be controllable and could be different. Rather than using active control, the AOA control unit employed passive control parts, namely spring, as mechanism.

The advantage of passive arrangement is twofold: It simulates the insect's flight control behavior more closely, and it reduces the complexity of the mechanical structure and control, and hence weight. The control in passive wing rotation mechanism only requires controlling the overall rotational angles, not like the active control situation in which the control of the instantaneous between the peaks is also required. On the other hand, active control must use precisely controlled motor, while passive control only needs to use mini servo motors like the ones often found in model aircraft. The simplifications might be beneficial to the design of future MAV.

The mechanism consists of wing, F/T sensor (on the wing root, shown in Figure 3 but 5), and wing rotation angle control housing. Wing rotating shaft which goes inside wing rotation control housing, is the extension of the wing root, and joins the middle of a lever. Each end of the lever is in contact with one end of each spring. And the other ends of the springs are fixed on the wing rotation angle control housing.

The passive wing rotation is realized in the following way. During up or down stroke, wing experiences aerodynamic force due to the surrounding air, as well as inertial force due to the angular acceleration. The centers of these forces don't lie on the wing rotational axis. Hence, a torque about the rotational axis by these forces is produced and consequently it makes the wing rotating. Two springs in the rotation angle control housing limit the degrees that the wing could rotate in either direction independently. By changing the stiffness in the spring, the angle of wing rotation shaft will change accordingly, hence the overall AOA..

In addition to the method employed to vary the spring tension mentioned above, changing spring is another way to change the spring tension therefore wing rotation and AOA. This method is applied when the spring tension required exceeds the maximum the spring could provide in the space restricted housing. Figure 4 illustrates the wing rotation control unit.

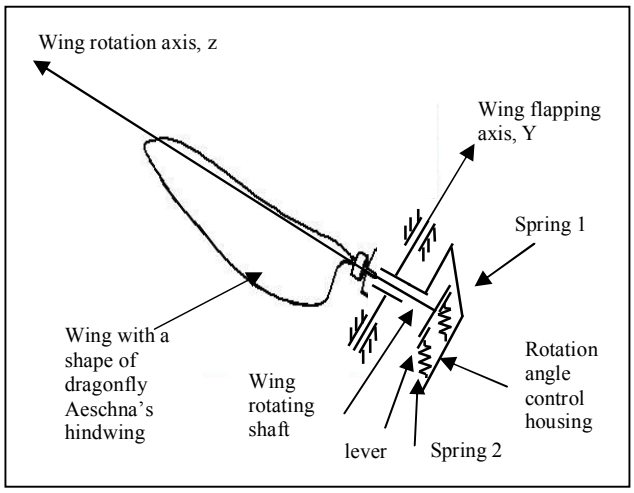

Figure 4. Wing Rotation Control Unit

2.1.4 Wing Design

The wing used in the test took a shape of Dragonfly, A*eschna juncea's* hind-wing(Norberg 1972), but enlarged about 11 times in both length and width dimension. The material used for making the wing veins is carbon fiber epoxy divinycell foam sandwich (CFEDFS) which has a 3.2mm divinycell foam layer in the middle and 12 *oz* carbon fiber on either side. The carbon fiber layer is so thin that the divinycell foam layer's thickness 3.2mm could be considered as the thickness of the sandwich. CFEDFS has the properties of being extremely light and rigid. Because of these properties, it was chosen to be the wing's vein structure. When actually making the wing, the patterned vein structure was cut out from a whole piece of CFEDFS, by using a bench saw. After vein structure was made, a membrane made of food wrapping plastic was glued onto the top of the vein structure.

2.2 Electrical System Design

The electrical system provides an accurate control for flapping frequency of the experimental device. It consists of one driving motor, one reduction gearbox, one digital coder, one servo amplifier, one power supplier and one personal computer program with Graphical User Interface (GUI) for motor speed control. High frequency chokes were used before the power is supplied to the motor. Most parts in electrical system are selected from Maxon Motor, a leading supplier of high precision drives and systems.

EC 45 blushless motor with 250 watts from Maxon was chosen to drive the system. The motor has the maximum speed of 11000rpm. The nominal operating voltage is 48v. The motor draws continuous current of 8.2 A at the speed of 5000 rpm. This motor provides a reliable driving source.

Planetary gear head GP 42C, also from Maxon, was chosen, which has output torque 3-15Nm and reduction ratio of 26:1. The gearbox transmits power stably. The only disadvantage is its mechanical noise. Extra insulation effort had to be spent to remove the noise. Digital encoder HP HEDS 6540, also from Maxon Motor was employed to detect the rotor's position and the rotating direction for the precise motor speed and position control.

4-Q-EC servo amplifier DEC 70/10 serves as control brain for the electrical driving system. It has the advantage of providing digital speed control as well as digital torque control. The control can be operated in both acceleration and braking directions. It is also supported by GUI in Windows operation system.

The power supply used in the current test bench is Parameters P4303, a dual-tracking DC power supply, which takes AC from the main and transforms it to DC. By combined two channels in series, it provides a variable voltage between 0 and 60 v and the total current output could reach 6 A. It has been found that it could offer sufficient power for the current experimental device.

Without using high frequency chokes, an audible sharp electrical noise could be generated from the motor. The high pitch noise was caused by the digitized motor supply power. By connecting 3 high frequency chokes between the 3 power cables to the motor and the servo amplifier the noise was eliminated.

A motor control program with GUI, specially written for Maxon Motor, was chosen to run the control operation. The flapping frequency in the present experiment is around 1 Hz. With the controllable accuracy of 0.016 Hz, the GUI control program is well suitable for the current experiment device. The schematic of the electrical system is illustrated in Figure 5.

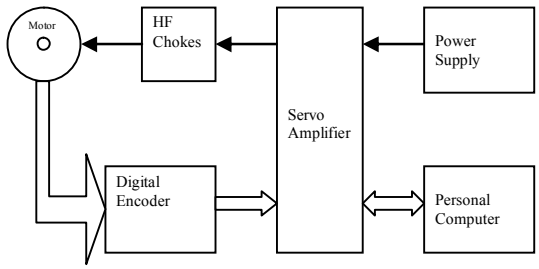

Figure 5. Schematic of Electrical System

2.3 Data Acquistion System

In the present experimental study, there are two kinds of data to be collected. One is the force and torque data from the 6-DOF sensor. The other is the wing rotational angle values measured by a Hall-effect sensor. Force/torque data recorded the force and torque at the wing root portion during flapping. Rotational angle values reflect the course of wing root.

A 6-DOF Nano 43 sensor from ATI was mounted between the wing root and the AOA control unit. The 6-DOF sensor collects the forces F_x, F_y, F_z and torque M_x, M_y, M_z, in x, y, z coordinate directions with the reference to the sensor. This reference is defined as follows. The origin is at the centre of sensor. z, is the direction pointing outwards from the centre of the sensor.

Data acquisition card used in the current device bridges the conditioned data and the computer central processing unit, where the data are converted from the voltages to readable force and torque. The data acquisition card employed in the current device is NI PCI-6221, an M series, fast yet low cost data acquisition card from National Instrument.

The personal computer used in this study is Pentium II 2.6 GHz with 1G Ram. It is found this computer is capable of carrying out the multi-tasks assigned to the experiments. It can simultaneously process the data collected from the 6-DOF sensor, run the speed control program for motor, and run the Matlab program for post-test data analysis.

The rotational angle of wing during the flapping motion was measured at the end of the rotating shaft. The measurement employs a Hall-effect sensor and a magnet. Hall-effect sensor is sensitive to magnetic field strength around it. A cylindrical magnet polarized at both ends was fixed at the end of the wing rotation shaft with its axis parallel to the axis of the shaft and having offset distance about 5 mm. The magnet rotates with the wing rotation. The Hall-effect sensor, whose working side facing one end of the magnet, was fixed at the position next to the magnet and 2 mm apart. When the wing rotates away from its neutral position, it carries the magnet away from its closest position to the Hall-effect sensor. The magnetic field detected in the sensor reduces gradually during the process. The rotation angle information collected in the Hall-effect sensor was displayed in the oscilloscope as voltages.

During calibration, a high speed camera was placed in front of the wing. The images captured by this camera were displayed on a second computer where the rotational angle was measured. While measuring the rotation angle, the corresponding voltage displayed on the oscilloscope was also recorded. A cubic polynomial curve fit was then developed to correlate the recorded voltages to the rotation angle.

The data collected from the 6-DOF sensor are based on the sensor coordinate system. Because the sensor is mounted on the wing root, it flaps and rotates with the motion of the wing root. To gain the aerodynamic force with respect to the ground, the data collected from the sensor must be converted to ground reference. The force and moment data with respect to the ground reference provide useful information for the design of MAV. This task was carried out in the post-test data process in Matlab. The schematic of the data acquisition system is illustrated in Figure 6.

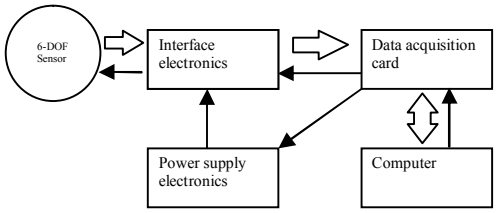

Figure 6. Schematic of the Data Acquisition System

3. Experimental Results and Discussion

The experiments were performed to elucidate the effectiveness of the current test bed in providing reliable data during the flapping motion. The results obtained in this study were compared to results obtained through simulation and on testing of live dragon flies. During testing, the flapping frequency was set at 1 Hz. Flapping amplitude was set at +/-52 degree with respect to the horizontal plane. Down stroke AOA was set to zero during the tests. During upstroke, AOA varied and was the result of combined effects of aerodynamic and inertial forces. It was found that the flexibility effects were negligible for the

current wing design and the AOA was measured at the end of wing rotating shaft. Experiments were conducted under two situations: wing with membrane and wing without membrane. Two sets of test data were collected. A Matlab program was written to process the collected data to obtain the aerodynamic force in ground reference. In the program, AOA, force/torque with membrane and force/torque without membrane were phase averaged first. By subtracting the data from the experiments carried out without membrane from the data with membrane, the effect of inertial was eliminated. The rationale for this assumption was that the membrane's contribution to the inertial forces was negligible. Finally a routine was written that converted the data from sensor reference to ground reference. The flow chart of this program is illustrated in Figure 7.

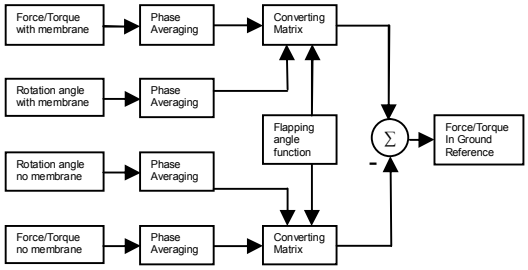

Figure 7. Flow Chart of post-test data analysis program

The results on force and moment data are illustrated in Figure 8 and Figure 9.

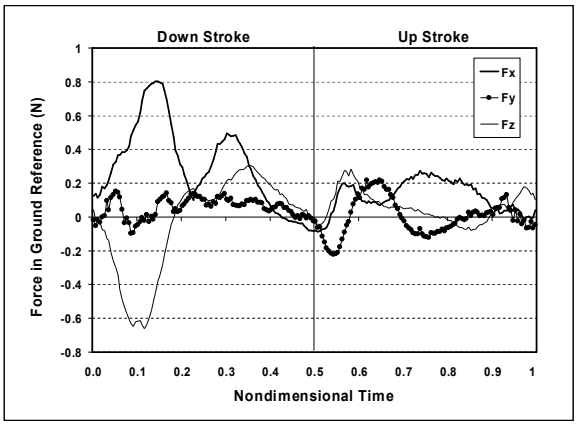

Figure 8. Test results for force data in ground reference

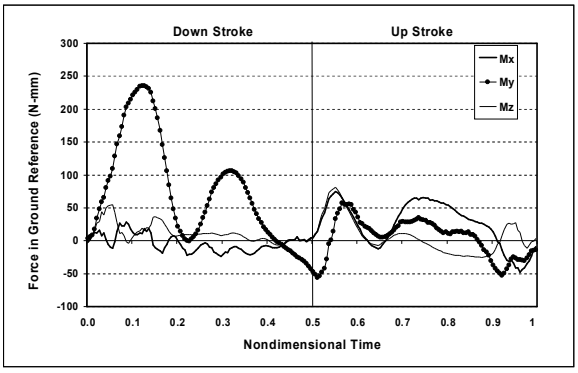

Figure 9. Test results for moment data in ground reference

Figure 10 illustrates the vertical lift force coefficient as a function of non dimensional time. The wing tip velocity, when wing passing its horizontal position, was used as the reference when vertical force coefficient was calculated.

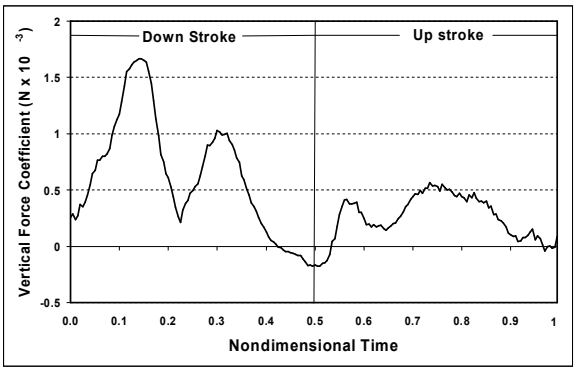

Figure 10. Experimental results for lift force coefficient

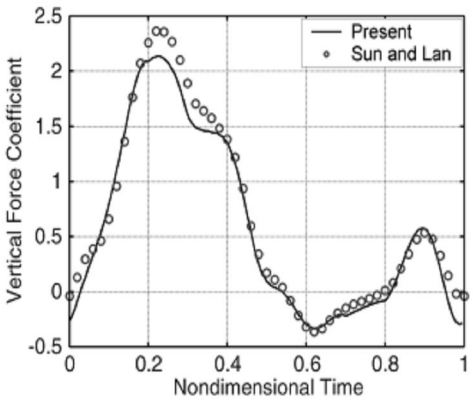

Figure 11 CFD simulations for lift. (Permitted copy from Young 2008)

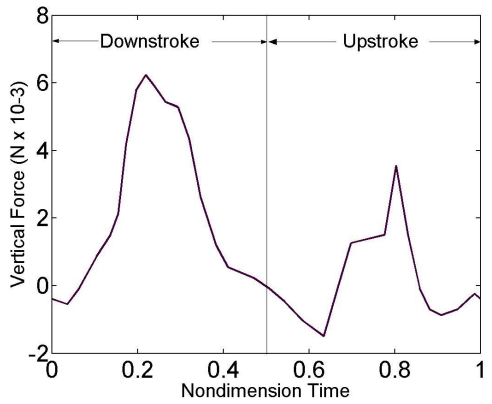

Figure 12 Calculated Vertical Force (reconstructed from Azuma 1985)

The results from the current work on lift coefficient were compared with CFD simulations [Young, 2008; Sun and Lan, 2004] in Figure 11 and the experimental work carried out on live dragonfly [Azuma A., Azuma S., *et.al* 1985] in Figure 12. This comparison indicates that both the pattern of the data during flapping and the magnitude of the lift coefficient match reasonably well. This clearly has demonstrated the correct functioning of the device in obtaining high quality test results.

4. Conclusion

An electro-mechanical test bench using passively rotating wing was successfully designed. The angle of attack during the upward and downward strokes can be independently controlled. This device is the first of its kind that incorporates both passive wing flapping motion and the ability to vary the angle of attack during the motion. The lift force and the lift data pattern phase-averaged in one flapping cycle were similar to the ones generated through computer simulations and based on the measurement from a live dragon fly. Our future work will present results that consider the effect of frequency of motion, flexibility of the wings and the effect of variation of AOA during the motion. It is expected that the current/future studies will shed fundamental information about the aerodynamic characteristics of the insect flight and this in turn can aid in the design and development of MAV.

References

[Azuma et al., 1985] A. Azuma and S. Azuma. Flight Mechanics of a Dragonfly. *Journal of Experimental Biology* 116(1): 79-107, 1985.

[Bergou et al.,] A.J Bergou et al., Passive wing pitch reversal in insect flight. *J.Fuid Mech.* vol. 591, pp.321-327, 2007.

[Dickinson and Gotz 1993] M.H. Dickinson and K.G Gotz. Unsteady Aerodynamic Performance of Model Wings at low Reynolds Numbers. *Journal of Experimental Biology*, Vol. 174(1), pp. 45-64, 1993.

[Dickinson, 1994] M.H. Dickinson. The Effects of Wing Rotation on Unsteady Aerodynamic Performance at Low Reynolds Numbers. *Journal of Experimental Biology*, Vol. 192(1), pp. 179-206, 1994.

[Lehmann, 2004] F.O Lehmann. Aerial locomotion in flies and robots: Kinematic control and aerodynamics of oscillating wings. *Arthropod Structure & Development*, Vol. 33(3), pp. 331-345, 2004.

[Lu et.al, 2006] Y.Lu, G.X Shen et.al, Dual Leading-Edge Vortices on Flapping wings. *Journal of Experimental Biology,* Vol. 209(24), pp. 5005-5016, 2006.

[Mayberry et.al, 2004] W.J.Maybury and F.-O. Lehmann The fluid dynamics of flight control by kinematic phase lag variation between two robotic insect wings. *Journal of Experimental Biology*, Vol. 207(26), pp. 4707-4726, 2004.

[Norberg, R. A. 1972]. "The pterostingma of insect wings an inertial regulator of wing pitch." J.comp. Physiol.(81): 9-22.

[Sane 2005] S.P Sane Induced airflow in flying Insects. A theoretical model of the induced flow. *Journal of Experimental Biology*, Vol. 209(1) , pp. 32-42, 2005.

[Sun and Lan, 2004] M. Sun, M. and S. L. Lan. A computational study of the aerodynamic forces and power requirements of dragonfly (Aeschna juncea) hovering. *Journal of Experimental Biology*, Vol. 207(11), pp. 1887-1901, 2004.

[Young, 2008] J.Young. Simulation and parameter variation of flapping-wing motion based on dragonfly hovering. *AIAA Journal* Vol.46, No.4, April 2008.

[Usherwood and Ellington 2002] J.R Usherwood and C. P. Ellington. The aerodynamics of revolving wings I. Model hawkmoth Wings. *Journal of Experimental Biology*, Vol. 205(11), pp. 1547-1564, 2002.

[Weis-Fogh, 1973] T. Weis-Fogh. Quick Estimates of Flight Fitness in Hovering Animals, Including Novel Mechanisms for Lift Production. *Journal of Experimental Biology*, Vol. 59 (1), pp. 169-230, 1973.